ASME Journal of Applied Mechanics
Online journal at:
https://asmedigitalcollection.asme.org/appliedmechanics

Osmotic Pressure Gradient Effects on Water Diffusion in Porous Rock: Can They Pervert Permeability Tests?

Zdeněk P. Bažant[1]
McCormick Institute Professor and W.P. Murphy Professor of Civil and Mechanical Engineering and Materials Science,
Northwestern University,
2145 Sheridan Road,
CEE/A135, Evanston, IL 60208
e-mail: z-bazant@northwestern.edu

Anh Tay Nguyen
Department of Mechanical Engineering,
Northwestern University,
2145 Sheridan Road,
Evanston, IL 60208

Generation of a large network of hydraulic cracks is of key importance not only for the success of fracking of shale but also for the recent scheme of sequestration of CO_2 in deep formations of basalt and peridotite, which are mafic and ultramafic rocks that combine chemically with CO_2. In numerical simulation of the creation of a fracture network in porous rock, an important goal is to enhance the rock permeability. The objective of this article is to calculate the effect of osmotic pressure gradients caused by gradients of concentration of the ions of Ca, Mg, Na, etc. on the effective permeability of the rock. The basic differential equations are formulated, and their explicit solutions for appropriate initial and boundary conditions are obtained under certain plausible simplifications. The main result is explicit approximate formulas for the critical time before which no water permeation through a test specimen can be observed. Depending on various parameters, this time can be unacceptably long, which is manifested as a zero water outflow. The solution may also explain the unreasonably small permeability values reported for some shales.
[DOI: 10.1115/1.4063030]

Keywords: osmotic pressures, ion concentration in pores, diffusion, permeability tests, critical time of water outflow, porous rocks, shale, basalt, peridotite, mafic rocks, hydraulic fracturing (fracking), deep CO_2 sequestration, computational mechanics, flow and fracture, hydraulics

1 Introduction

Hydraulic fracturing of shale, also known as fracking (or fraccing, frac) is used to induce crack growth and branching [1,2]. Although this technology has been remarkably successful, its fracture mechanics is not yet completely understood, which means that further significant advances should be possible [3–5]. Importantly, emulation of the frac technology ought to be also helpful in designing the technology of sequestration of CO_2 in deep formations of mafic and ultramafic rocks, particularly basalt, peridotite, and basalt with peridotite inclusions (these are dark igneous ferromagnesian rocks, with a high or very high content of iron and magnesium, which combine CO_2 chemically).

One aspect that has not been adequately explored is the quantitative studies on the effect of the gradients of osmotic pressures on the growth of hydraulic crack system in deep formations of porous rocks. Gradients of the concentration of alkali ions of Ca, Mg, and Na, which give rise to gradients of osmotic pressures, are always present in rocks, and the basic equations governing these osmotic pressures have been well known for a long time. Valuable information on the effects of osmotic pressure gradients is found in many studies [6–11]. Some of these studies were purely phenomenological, while some presented equations with their semi-intuitive interpretation. Remotely relevant are many other papers, which discussed the effects of Darcian permeability, disjoining pressure, flowback from fracking, effect of confining stress on crack width and permeability of shale, permeability enhancement at a fault, role of salt ions in serpentized peridotites, and permeability increase due to Knudsen diffusion and molecular slippage (Klinkenberg effect); see, e.g., Refs. [11–20]. Sarouta and Detournay [21] used the Laplace transform to solve the linear diffusion problem of chemoporoelasticity with osmotic pressure gradients. However, their approach does not allow setting up explicit expressions for the depth and times of diffusion penetration fronts.

The purpose of this article is to provide complete mathematical formulation of the initial boundary value problem of differential equations for water diffusion in porous rock under combined water pressure and osmotic pressure gradients. Approximate analytical solutions for the critical time, up to which there is no outflow of water at the unpressurized face, and the cumulative water discharge are derived for the one-dimensional flow across a wall or along a drilled core. The explicit formulas reveal the effects of wall thickness, water pressure difference, osmotic pressure difference, and diffusivity of porous rock on the rock permeability, which play a major role in the development of the hydraulic crack system in shale or in mafic rocks. For a review of the governing equations of water flux in saturated rock, see the study by Leng et al. [22].

A particular purpose of this article is to explain why the osmotic gradients must be considered in evaluating permeability tests. In a study by Heller et al. [13], examining the effects of confining

[1]Corresponding author.
Manuscript received June 18, 2023; final manuscript received July 17, 2023; published online August 7, 2023. Assoc. Editor: Ruike Renee Zhao.

stress and pore pressure on matrix permeability, the permeability tests of different shale core plugs gave a wide range of permeability values spanning over many orders of magnitudes, indicating some unreasonably small values, while some other tests even gave zero effective permeability. Here, we explain it mathematically by analyzing in a simplified way the osmotic effects under the assumption of low mobility of calcium, potassium, sodium, and chloride ions in the pores of rock.

2 Basic Equations of Coupled Water and Ion Diffusion

Let P be the total pressure in pore water in the rock (dimension Pa) and c be the concentration of ions, such as Na^+, Cl^-, and Ca^{2+} (mol/m^3), in the pore water. Then, as known from electrochemistry, the water flux, q_w (m/s) in 1D (one dimension, with coordinate x), is given by [22]

$$q_w = \frac{k}{\mu}\left(-\nabla P + \chi \nabla \Pi\right), \quad \nabla \Pi = \nu R T \nabla c \tag{1}$$

where $\nabla = \partial/\partial x$ (in 1D), k = water permeability of shale or basalt (m^2), μ = kinematic viscosity (Pa · s), T = absolute temperature (K) (considered here to be uniform), R = universal gas constant (8.314 J/mol · K), $\Pi = \nu R\ T\ c$, c = concentration of ions in the solvent, i.e., water electrolyte (mol/m^3), ν = stoichiometric coefficient = number of ions in water per mole of solute ions (for sodium, NaCl = $Na^+ + Cl^-$, $\nu = 2$), and χ = osmotic efficiency ($0 < \chi < 1$), for shale typically $\chi = 0.04$. $\chi = 1$ represents perfectly immobile ions, which is equivalent to a perfect semipermeable membrane (note that from a thermodynamic standpoint, one might better introduce the ion activity coefficient but due to the dilute nature of pore fluid, even in ultramafic rocks, this coefficient is close to unity, which allows using the concentration as one basic variable). In addition, the ion concentration amalgamates the contributions of different species of ions of Ca, Mg, Na, …, which is a frequently used approximation. It would be an unnecessary complication to consider each species separately.

The first term of Eq. (1) represents Darcy law, which has a negative sign in front because water flows from a higher to a lower pressure. The second term, the osmotic flow, has a positive sign in front because water flows from a lower to a higher concentration of the solute ions. The companion equation for flux q_s (dimension $mol/m^2 \cdot s$) of the solute (i.e., ions) is

$$q_s = (1-\chi)\left(-D_e \nabla c + c q_w\right) \tag{2}$$

where the first term represents Fick's law [23] because the ions move within the solute randomly, like in an ideal gas, as shown by van't Hoff in 1887 [24,25] (the first Nobel Prize in Chemistry). The second term represents advection, i.e., the drag of ions by moving water. D_e is the intrinsic diffusion coefficient of ions (m^2/s) in water. Substitution of Eq. (1) into Eq. (2) yields:

$$q_s = (1-\chi)\left[-\frac{k}{\mu} c \nabla P + \left(\frac{k}{\mu} r c - D_e\right)\nabla c\right], \quad r = \chi \nu R T \tag{3}$$

The condition of volume conservation of pore water is

$$\varphi \frac{\partial w}{\partial t} = -\nabla q_w \tag{4}$$

where w = pore water volume per cubic meter of rock (shale or basalt) and φ = porosity of rock. Substituting Eq. (1) for q_w, and by setting $dw = -C_t dP$, we have the diffusion equation for water content as affected by ion osmosis (t = time):

$$\frac{\partial P}{\partial t} = \frac{k}{\varphi C_t \mu}\left(\nabla^2 P - r \nabla^2 c\right) \tag{5}$$

where C_t = total compressibility of pore water, $C_t = C_\varphi + C_L$ = sum of the compressibilities of pore space and of pore fluid phase, $1/C_\varphi = \varphi(\partial\varphi/\partial P)$, $1/C_L = \rho(\partial\rho/\partial P)$, and ρ is the mass density of water. It may be noted that Eq. (4) is assumed to indirectly account for the net result of dissolution and precipitation of pore wall material, and ignores the possibility of producing a new material such as brucite in the case of ultramafic rocks.

The condition of conservation of the number of ions is

$$\varphi \frac{\partial c}{\partial t} = -\nabla q_s \tag{6}$$

By introducing Eq. (3), we get a diffusion equation for ion concentration as affected by pore pressure:

$$\varphi \frac{\partial c}{\partial t} = (1-\chi)\left\{\frac{k}{\mu}\nabla(c \nabla P) - \nabla\left[\left(\frac{k}{\mu} r c - D_e\right)\nabla c\right]\right\} \tag{7}$$

Supplemented by the initial and boundary conditions, Eqs. (5) and (7) define the initial-boundary value problem for P and c as functions of x and t. Because of the term $c\nabla P$, describing the ion advection driven by water pressure gradient, the problem is nonlinear, except when advection is neglected (as done here).

Unless externally introduced, the electrical potential gradients need not be considered because the positive and negative ions, such as Na^+ and Cl^-, form double layers at pore surfaces, which are electrically neutral. One might also question whether the disjoining pressures in adsorbed water in nanopores, which can exceed 100 MPa, should be considered. They should not because unlike in creep behavior of unsaturated concrete, they do not play a role in macroscopic diffusion in saturated concrete [26], which must be similar for rock.

Some studies [13] inferred from test results a significant effect of confining pressure on permeability. In similarity to concrete [26], we do not consider this effect since the confining pressure can hardly reduce the pore width by a ratio much bigger than the overall strain in concrete, i.e., less than 1%, which cannot cause a major decrease of permeability. Change of pore width by an order of magnitude cannot be achieved by externally applied pressure since a local pore wall crushing is not observed.

3 Approximate Solution of Permeability of Porous Rock Between Two Parallel Planar Faces or Along a Drilled Core

To obtain an approximate solution, we need to convert the initial boundary value problem of differential equations to an initial-value problem for a system of ordinary differential equations. The way to do it is to assume realistic shapes for the distributions of pressure and concentration. Parabolic arcs serve this purpose well. It suffices to write the conditions of balance of fluxes at the ends of parabolic arcs and the conditions of overall mass balance. These conditions have the form of ordinary differential equations.

Replacing the error function profile of 1D linear diffusion equation with a parabolic profile has long been known to give a good approximation. In fact such an approximation is necessary to define the front of pressure penetration because the error function, which is the exact solution of the diffusion equation, gives nonzero pressures all the way to infinite distance (which is ignored since the far-away pressures are extremely small). This is a well-known paradox of the diffusion theory. However, its exact resolution is too complex and unnecessary for practical purposes; therefore, the parabolic approximation for the depth of penetration of pressure front is generally accepted.

Consider two parallel planar faces of shale or basalt core, at distance h, both normal to axis. Face 1 ($x = 0$)3 is exposed to water of pressure P_1, maintained constant. At face 2, the pressure is at $t = 0$ raised suddenly to P_2 ($P_2 > P_1$) and then maintained constant. The concentration of ions in the water of both faces is c_w and is, in general, different from the initial ion concentration c_0 in the pore water. We consider that the latter to be larger, i.e., $c_0 > c_w$.

At the pressurized face (face 2), both the water pressure gradient and the opposite ion concentration gradient cooperate in pulling

water into the specimen (Fig. 1). At the unpressurized face (face 1), the outflow faces the opposite situation—the two gradients compete. The water pressure gradient drives the water out, while the ion concentration gradient pulls the water in. The resulting water flow can be inward or outward.

To simplify analysis, we neglect the ion advection term cq_w, which is the only source of nonlinearity in the equation system (this follows from noting that the material usually acts as a semi-permeable membrane). Further we assume that a steady-state linear profile of water pressure P (a limit case of a parabola) will get established before the profile of ion concentration c begins to change appreciably. There are two reasons for that:

(1) The pore water is relatively "stiff" and the solute of ions is relatively "soft", i.e., a small change in the pore water content causes a large change in water pressure P, while a small change in ion concentration c leads to only a small change in osmotic pressure Π because the ions behave like an ideal gas (van't Hoff [23]), which is much more compressible than the porous solid.
(2) The ions in shale or mafic rock are strongly attracted to the pore surfaces, and so their mobility within porous rock (as well as concrete) is very small, far smaller than the mobility of water through rock pores (as indicated by $\chi = 0.96$). In view of the latter, can we consider the ions in rock to be immobile? For some purposes—yes, but not in the differential equation.

At the end face of the test cylinder (a core), there is initially a jump $\Delta c = c_0 - c_w$, which means that $\nabla\Pi$ is infinite (a delta function spike). If ion mobility did not reduce this jump to a small gradient, water would be flowing into the rock forever (like through a desalination membrane), i.e., no water would ever flow out. Therefore, the ions must have at least some mobility.

The pressure difference $P_2 - P_1$ across the specimen does not imply water to flow into face 1 because of the second flow term in the water flow equation (2), driven by the osmotic pressure gradient corresponding to ion concentration gradient. Initially, at $t = 0$, there is a concentration jump $\Delta c = c_0 - c_w$ (or infinite delta function spike $|\nabla c|$) at both rock surfaces (just like in an osmotic membrane for desalination). This osmotic effect pulls water at the end face into the shale or basalt (recall that water flows from lower to higher c). Since $|\nabla c|$ next to the surface decreases from ∞, the inward water flux component due to ∇c at face 1 will always initially overpower the outward water flux component due to ∇P, which is finite. If the ions were immobile, and the inward water flow would persist forever (like in a perfect desalination membrane). So we see again that it is necessary to assume the ions to have some degree of mobility.

As the ion concentration drop penetrates into the shale or basalt, the inward flux component will eventually, at a certain time t_{cr}, become smaller than the outward one, and only after t_{cr}, the water will start exiting through face 1. The fronts of the ion concentration drop propagate inward from both sides. Depending on whether the fronts meet in the middle, our simplified solution needs to distinguish two phases of behavior.

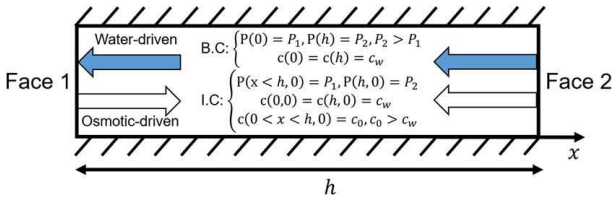

Fig. 1 A shale core of initial ion concentration c_0, pore pressure P_1, and thickness h is subjected to water pressure P_1 at face 1 and water pressure P_2 at face 2 ($P_2 > P_1$). The ion concentration of water at both faces is c_w ($c_0 > c_w$). The dark and the white arrows represent the water flux due to water pressure gradient and osmotic pressure gradient, respectively.

3.1 Phase I—Thick Enough Wall. To obtain a simple explicit estimate of t_{cr}, we neglect, according our two assumptions, the advection term cq_w in Eq. (2). This gives the simple diffusion equation:

$$q_s = -(1-\chi)D_e \nabla c \tag{8}$$

for which the profile of the drop in c at any time $t > 0$ can be closely approximated by a parabolic arc (Fig. 2) (the dimension of D_e is m^2/s). Let $x = s$ be the depth of penetration of the ion diffusion front, which represents the distance from face 1 ($x = 0$) to the apex of the parabolic profile. The ion mass loss between the face and the mid-thickness $h/2$ is $\varphi(c_0 - c_w)(1/3)$ s (per unit cross section area), and the concentration gradient at the end face is $(c_0 - c_w)/(s/2)$. The profile being fixed, we only need to satisfy the condition of overall balance of ion mass. This means that the flux of ions, $q_s|_{x=0}$, into end face 1 must be equal to the rate of change of the total mass of ions. Hence, in view of Eq. (8),

$$[q_s]_{x=0} = -\varphi \frac{c_0 - c_w}{3}\frac{\mathrm{d}s}{\mathrm{d}t} + (1-\chi)D_e \frac{c_0 - c_w}{s/2} = 0 \tag{9}$$

The solution of this differential equation for initial condition $s = 0$ at $t = 0$ gives the time to reach depth s:

$$t = \frac{\varphi s^2}{12(1-\chi)D_e} \quad (\text{if } s \le h/2) \tag{10}$$

To calculate s_{cr}, we must satisfy the water volume balance, Eq. (1). Since the shapes of profiles of P and c are considered as fixed, we can do that only in the overall sense for one half of the wall. The average pressure gradient over the whole wall is $(P_2 - P_1)/h$. However, what matters is the pressure gradient ∇P at the outflow face 1 ($x = 0$). At this face, we apply an empirical factor β (> 1) to increase ∇P to $\beta(P_2 - P_1)/h$ because at face 1, ∇c opposes the outflow, while at face 2 ($x = h$), it assists the inflow (Fig. 3). Therefore, the pressure gradient at face 1 must be at least a little greater than that at the opposite face.

From mass conservation principle, the pressure-driven flowrate of water volume into face 1, $(-k/\mu)\beta(P_2 - P_1)/h$, must be equal to the osmotic (i.e., concentration driven) flowrate of water volume, $(k/\mu)\chi\nu RT\,(c_0 - c_w)/(s/2)$, for a parabolic ion concentration profile (with $s \le h$),

$$[q_w]_{x=0} = -\frac{k}{\mu}\frac{\beta(P_2 - P_1)}{h} + \frac{k}{\mu}\chi\nu RT\frac{c_0 - c_w}{s/2} = 0 \tag{11}$$

Together with Eq. (10), this gives the critical s and t at which the outflow at face 1 begins:

$$\boxed{s_{cr} = \alpha_c \frac{h}{2},\ \alpha_c = 4\chi\nu RT\frac{c_0 - c_w}{\beta(P_2 - P_1)}} \quad \text{if } \alpha_c < 1 \tag{12}$$

$$\boxed{t_{cr} = \frac{\nu s_{cr}^2}{12(1-\chi)D_e}} \tag{13}$$

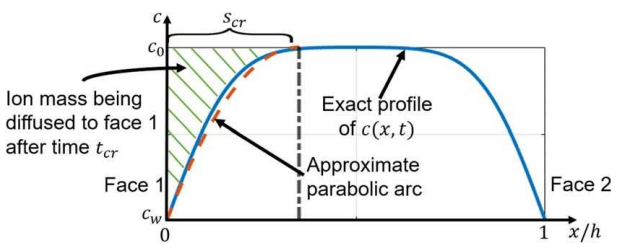

Fig. 2 Distribution of ion concentration across thick enough wall (or along a long enough drilled core) approximated by parabolic segments

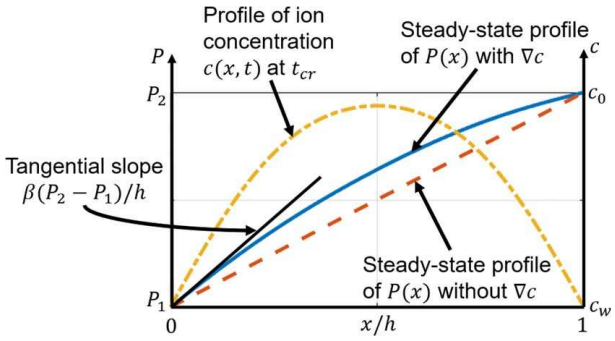

Fig. 3 Steady-state linear profile of water pressure (dashed line) and small deviation from that profile (solid curve) caused by ion distribution (dashed parabola)

Based on the present simplification, for times $t \le t_{cr}$ after pressurization of end face 2, no water outflow can be observed at face 1.

This may have tantalizing implication for the scheme of CO_2 sequestration in deep ultramafic rocks. If t_{cr} exists for the crack network to be created and is greater than the time needed for carbon to be consumed by precipitation of carbonates, e.g., $MgCO_3$ or $CaCO_3$, then no carbon would actually get sequestered.

As marked in Eq. (12), the present simplified solution is not valid when s_{cr} becomes greater than the half thickness of the wall, $h/2$. The reason is that a similar profile of an ion concentration drop advances in the negative x direction from the opposite wall surface. When it meets in the center of wall with the profile advancing from face 1 in the positive x direction, the profile can no longer advance; rather, its magnitude decreases (Fig. 4).

3.2 Phase II—Thin Enough Wall. The fronts of ion concentration drops are spreading from both faces. For simplicity, we assume both fronts to meet at mid-thickness $x = h/2$, which is at the time:

$$t^* = \frac{\varphi h^2}{48(1-\chi)D_e} \tag{14}$$

After t^*, the ion concentration profile may be considered to consist of two opposite parabolas with the apex at distance $h/2$ from either face (Fig. 4). Let $c = c(t)$ represent the ion concentration at the apex located now at the center. For the parabolic profile, the ion content within one half of the wall thickness is $(2/3)\varphi(c - c_w)(h/2)$, and its rate must equal the outflow of ions at face 1, which is $-(1-\chi)D_e(c - c_w)/(h/4)$. This yields for $c(t)$ the differential equation

$$\varphi \frac{dc}{dt} = -\frac{12(1-\chi)D_e}{h^2} \tag{15}$$

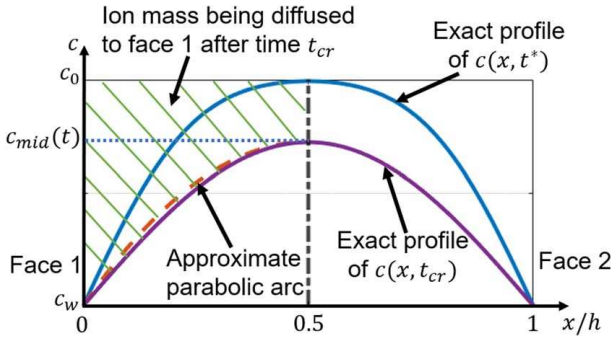

Fig. 4 Subsequent distributions of ion concentration, approximated as parabolas, in a thin-enough wall (or short enough drilled core)

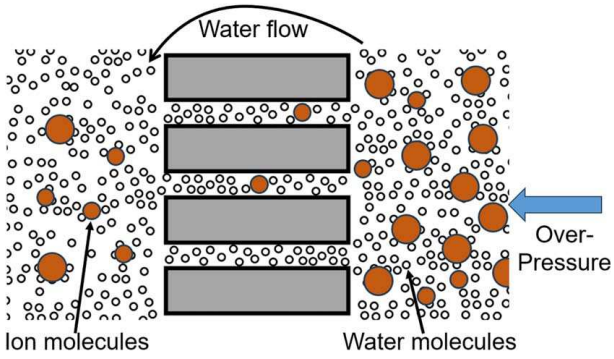

Fig. 5 Schematic diagram of small and large ion molecules (solid circle) of various species and of water molecules (empty circles), forced to pass through narrow pores by an applied pressure after critical time t_{cr}

Its solution for the initial condition $c = c_o$ at $t = t^*$ is given as follows:

$$c(t) = (c_0 - c_w)e^{-[12(1-\chi)D_e/(\varphi h^2)](t-t^*)} + c_w \tag{16}$$

The condition of zero water outflow q_w at face 1 is

$$[q_w]_{x=0} = -\frac{k}{\mu}\frac{\beta(P_2-P_1)}{h} + \frac{k}{\mu}\chi\nu RT\frac{c(t)-c_w}{h/4} = 0 \tag{17}$$

After substituting Eq. (16) for $c(t)$, we obtain

$$\boxed{t_{cr} = t^* + \frac{\varphi h^2}{12(1-\chi)D_e}\ln\alpha_c} \quad \text{if } t_{cr} \ge t^*,\ \alpha_c > 1 \tag{18}$$

If $\alpha_c \le 1$, phase I (Eqs. (10)–(12)) applies.

The transition from Eq. (13) to Eq. (18) occurs here with discontinuous derivative $dt_{cr}/d\alpha_c$. The reality is doubtless a continuous transition. This may be achieved by empirical partition of unity satisfying proper asymptotic conditions, e.g., by setting

$$t_{cr} = \eta_c\, t_{cr}^{\text{Eq. (13)}} + (1-\eta_c)\, t_{tcr}^{\text{Eq. (18)}} \tag{19}$$

$$\text{where} \quad \eta_c = \frac{1}{2}\left[1 - \tanh\left(\frac{\alpha_c}{\alpha_0}\right)\right] \tag{20}$$

for all α_c; here, tanh is an empirical function varying from 0 to 1, providing a smooth transition from phase I and II, and α_0 is an empirical parameter controlling the spread or sharpness of the transition.

Before t_{cr}, water flows at face 1 inward into the shale or basalt, while after t_{cr}, it flows from face 1 outward. When the water flows toward a lower ion concentration, this is called the *reverse osmosis* (Fig. 5), which is enforced by a sufficiently high fluid pressure difference. Like in membrane desalination, the key to achieve positive permeability is to apply high enough pressure to induce reverse osmosis at the low pressure face.

Note that the specimen thickness h has a big effect—the time to outflow depends on the h quadratically.

3.3 Water Discharge at Face 1 After Critical Time. *Thick Wall:* From Eq. (10), we have

$$s = \sqrt{\frac{[12(1-\chi)D_e t]}{\varphi}} \tag{21}$$

By substituting it into Eq. (11), we obtain the evolution of the rate, q_w, of water discharge from face 1 after t_{cr}, per unit area of the face

(dimension m, i.e., m^3 of water per m^2 of face 1 area):

$$|q_w(t)| = A - \frac{1}{2}Bt^{-1/2} \tag{22}$$

$$\text{where} \quad A = -\frac{k}{\mu}\frac{\beta(P_2 - P_1)}{h}, \quad B = -\frac{\chi RT(c_0 - c_w)}{\sqrt{[3/(4\varphi)](1-\chi)D_e}} \tag{23}$$

By integrating over time with the initial condition $q_w = 0$ at $t = t_{cr}$, we obtain the cumulative discharge:

$$\bar{w}(t) = \int_{t_{cr}}^{t} |q_w(t')|\mathrm{d}t' = |A|(t - t_{cr}) - |B|(\sqrt{t} - \sqrt{t_{cr}}) \tag{24}$$

At $t = t_{cr}$, the water discharge begins asymptotically at zero rate, $\mathrm{d}\bar{w}/\mathrm{d}t = 0$ (Fig. 6).

Thin Wall: By substituting Eq. (16) into Eq. (17) and integrating from t_{cr} to t, we get the cumulative outflow at face 1:

$$\bar{w}(t) = \int_{t_{cr}}^{t} |q_w(t')|\mathrm{d}t' = |A|(t - t_{cr}) - \frac{G}{H}\left[e^{-H(t-t^*)} - e^{-H(t_{cr}-t^*)}\right] \tag{25}$$

$$\text{where} \quad G = -\frac{k}{\mu}\frac{4\chi\nu RT}{h}(c_o - c_w), \quad H = \frac{12(1-\chi)D_e}{\varphi h^2} \tag{26}$$

4 Comments on Methods of Permeability Measurement and Numerical Solution

One way to measure permeability in the presence of osmotic effects is by fitting data on the cumulative inflow $w(t) = \int q_w \, \mathrm{d}t$ at face 1, using a nonlinear optimization subroutine such as the Levenberg Marquardt algorithm, with A, B or G, H and t_{cr} as unknowns whose optimum values minimize the sum of squared errors.

It may seem preferable to conducts permeability tests in which $c_w = c_0$. This would mean measuring the ion concentration (or osmotic pressure) within the rock core in advance, and then conducting the permeability test using water of the same concentration on both end faces of the core. In that case, the osmotic effects would get eliminated, and the permeability test could be conducted in the normal way. However, measuring c_0 is not easy. It may require permeability tests at different $P_2 - P_1$, which would offset the gain from knowing c_0. The pulse decay method has generally been considered as a more effective, less time consuming, way to measure permeability. It should be possible to adapt the present analysis to that method.

If ion advection by water flow is not negligible, or if complicated geometries of fracture networks are considered, a numerical solution will be necessary, which is relegated to a subsequent article. A small advection term might be best taken into account by sequential analysis, in which the advection term are evaluated and used as given constants in the next numerical simulation. This will preserve the linearity of the equation system.

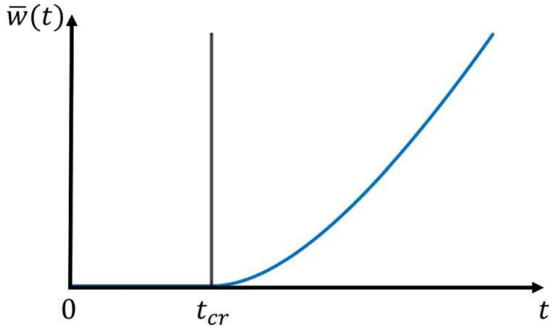

Fig. 6 Water discharge $\bar{w}(t)$ evolution at face 1 as a function of time t

5 Broader Practical Implications

The present analysis established a simple approximate method for a realistic testing of water permeability in the presence of osmotic pressure gradients. There are various consequences for shale fracking and for the CO_2 sequestration in mafic rocks.

There are also various consequences for concrete permeability and durability. However, because of the time constraints of the special issue for which this article has been written, numerical study of such practical consequences must be relegated to a follow-up paper.

6 Conclusions

(1) The complete mathematical formulation of the initial boundary value problem of differential equations for diffusion under water pressure and osmotic pressure gradients, which is presented here, can be analytically solved based on approximating the distributions of water and osmotic pressures by parabolic arcs.
(2) The fact that some tests of shale cores give a zero permeability or unreasonably small permeability values is not surprising. The likely explanation is the effect of osmotic pressure gradients as analyzed here.
(3) The ions of Ca, Mg, and Na, forming an electrically neutral double layer at pore surfaces, are considered as immobile in comparison to water. This is a usual approximation.
(4) Explicit formulas for one-dimensional diffusion across a wall or along a drilled core are derived, thanks to the simplification of the distributions of pore water pressure and osmotic pressure by parabolic segments, yielding easily solvable ordinary differential equations expressing the conditions of overall balance of mass and fluxes for each parabolic segment.
(5) Different explicit formulas are obtained for thin and thick walls, depending on whether the diffusion fronts do or do not meet at the center. Asymptotic matching provides a smooth transition between these two cases.
(6) Depending on the water pressure difference and osmotic pressure difference, there exist a critical time up to which there is no outflow of water at the unpressurized face. The critical time can tend to infinity, which means that no outflow is observed.
(7) The critical time increases with the ion concentration difference and decreases with the water pressure difference.
(8) The outflow of water from the unpressurized face is, after the critical time, a nonlinear function of pressure difference and ion concentration difference between the opposite faces. This causes apparent variation of effective permeabilities.
(9) A long critical time may explain why some tests of shale showed zero permeability, and why the reported permeabilities of shale ranged over many orders of magnitudes, indicating some unreasonably small values.
(10) The osmotic pressure gradient effects are of interest for both fracking of shale and sequestration of CO_2 in deep formations of mafic and ultramafic rocks (basalt and peridotite). Doubtless they are also relevant to water permeation through concrete.

Acknowledgment

This work was supported as part of the Center on Geo-Process in Mineral Carbon Storage, an Energy Frontier Research Center (EFRC) funded by the US Department of Energy, Office of Science, Basic Energy Sciences at the University of Minnesota under award DE-SC0023429. Dr. Pouyan Asem of the University of Minnesota is thanked for very helpful comments.

Conflict of Interest

There are no conflicts of interest.

Data Availability Statement

The datasets generated and supporting the findings of this article are obtainable from the corresponding author upon reasonable request.

References

[1] Bažant, Z. P., Salviato, M., Chau, V. T., Viswanathan, H., and Zubelewicz, A., 2014, "Why Fracking Works," ASME J. Appl. Mech., **81**(10), p. 101010.

[2] Rahimi-Aghdam, S., Chau, V.-T., Lee, H., Nguyen, H., Li, W., Karra, S., Rougier, E., Viswanathan, H., Srinivasan, G., and Bažant, Z. P., 2019, "Branching of Hydraulic Cracks Enabling Permeability of Gas or Oil Shale With Closed Natural Fractures," Proc. Natl. Acad. Sci. U. S. A., **116**(5), pp. 1532–1537.

[3] Chau, V. T., Li, C., Rahimi-Aghdam, S., and Bažant, Z. P., 2017, "The Enigma of Large-Scale Permeability of Gas Shale: Pre-existing or Frac-Induced?," ASME J. Appl. Mech., **84**(6), p. 061008.

[4] Bazant, Z. P., and Tabbara, M. R., 1992, "Bifurcation and Stability of Structures With Interacting Propagating Cracks," Int. J. Fracture, **53**(3), pp. 273–289.

[5] Nguyen, H. T., and Bažant, P. Z., 2022, "Osmotic Ion Concentration Control of Steady-State Subcritical Fracture Growth in Shale," Proceedings of the 56th U.S. Rock Mechanics/Geomechanics Symposiums, Santa Fe, New M, June 26–29, Paper No. ARMA–2022–0830.

[6] Horseman, S., Harrington, J., and Noy, D., 2007, "Swelling and Osmotic Flow in a Potential Host Rock," Phys. Chem. Earth, Parts A/B/C, **32**(1), pp. 408–420.

[7] Marine, I. W., and Fritz, S. J., 1981, "Osmotic Model to Explain Anomalous Hydraulic Heads," Water. Resour. Res., **17**(1), pp. 73–82.

[8] Morsy, S., and Sheng, J. J., 2014, "Effect of Water Salinity on Shale Reservoir Productivity," Adv. Petroleum Explor. Dev., **8**(1), pp. 9–14.

[9] Takeda, M., Hiratsuka, T., Manaka, M., Finsterle, S., and Ito, K., 2014, "Experimental Examination of the Relationships Among Chemico-Osmotic, Hydraulic, and Diffusion Parameters of Wakkanai Mudstones," J. Geophys. Res.: Solid Earth, **119**(5), pp. 4178–4201.

[10] Zhou, Z., Teklu, T., Li, X., and Hazim, A., 2018, "Experimental Study of the Osmotic Effect on Shale Matrix Imbibition Process in Gas Reservoirs," J. Natural Gas Sci. Eng., **49**, pp. 1–7.

[11] Barclay, L. M., Harrington, A. H., and Ottewill, R. H., 1972, "The Measurement of Forces Between Particles in Disperse Systems," Kolloid-Zeitschrift und Zeitschrift für Polymere, **250**(7), pp. 655–666.

[12] Wu, W., Reece, J. S., Gensterblum, Y., and Zoback, M. D., 2017, "Permeability Evolution of Slowly Slipping Faults in Shale Reservoirs," Geophys. Res. Lett., **44**(22), pp. 11368–11375.

[13] Heller, R., Vermylen, J., and Zoback, M., 2014, "Experimental Investigation of Matrix Permeability of Gas Shales," AAPG Bull., **98**(5), pp. 975–995.

[14] Neuzil, C. E., and Provost, A. M., 2009, "Recent Experimental Data May Point to a Greater Role for Osmotic Pressures in the Subsurface," Water. Resour. Res., **45**(3).

[15] Neuzil, C., 2019, "Permeability of Clays and Shales," Annu. Rev. Earth. Planet. Sci., **47**(1), pp. 247–273.

[16] Neal, C., and Stanger, G., 1985, *Past and Present Serpentinisation of Ultramafic Rocks; an Example From the Semail Ophiolite Nappe of Northern Oman*, Springer Netherlands, Dordrecht, pp. 249–275.

[17] Macdonald, A., and Fyfe, W., 1985, "Rate of Serpentinization in Seafloor Environments," Tectonophysics, **116**(1), pp. 123–135.

[18] Etheridge, M. A., Wall, V. J., and Vernon, R. H., 1983, "The Role of the Fluid Phase During Regional Metamorphism and Deformation," J. Metamorphic Geol., **1**(3), pp. 205–226.

[19] Dickey, J. S., 1972, "A Primary Peridotite Magma-Revisited: Olivine Quench Crystals in a Peridotite Lava," *Studies in Earth and Space Sciences*, Geological Society of America, Boulder, CO, pp. 289–298.

[20] Wicks, F. J., Whittaker, E. J. W., and Zussman, J., 1977, "An Idealized Model for Serpentine Textures After Olivine," Can. Mineral., **15**(4), pp. 446–458.

[21] Sarouta, J., and Detournay, E., 2011, "Chemoporoelastic Analysis and Experimental Validation of the Pore Pressure Transmission Test for Reactive Shales," Int. J. Rock Mech. Mining Sciences, **48**(5), pp. 759–772.

[22] Leng, J., Lin, X., and Wang, L., 2021, "Effects of Osmosis on Darcy Flow in Shales," Energy. Fuels., **35**(6), pp. 4874–4884.

[23] Fick, A., 1855, "V. On Liquid Diffusion.," London, Edinb. Dub. Phil. Mag. J. Sci., **10**(63), pp. 30–39.

[24] van't Hoff, J. H., 1887, "The Role of Osmotic Pressure in the Analogy Between Solutions and Gases.," Z. für physikalische Chemie, **1**, pp. 481–508.

[25] Atkins, P., de Paula, J., and Keeler, J., 2002, *Atkins' Physical Chemistry*, 11th ed., Oxford University Press, Walton Street, Oxford.

[26] Bazant, Z., and Jirásek, M., 2018, *Creep and Hygrothermal Effects in Concrete Structures*, 1st ed., Vol. 225, Springer, Dordrecht, The Netherlands, p. 1.